

Evolution of the temporal slope density function for waves propagating according to the inviscid Burgers equation

Michael B. Muhlestein^{1,a)} and Kent L. Gee²

¹*Applied Research Laboratories and Department of Mechanical Engineering, The University of Texas, Austin, Texas 78713-8029, USA*

²*Department of Physics and Astronomy, Brigham Young University, Provo, Utah 84602, USA*

(Received 26 March 2015; revised 15 December 2015; accepted 17 January 2016; published online 23 February 2016)

An exact formulation for the evolution of the probability density function of the time derivative of a waveform (slope density) propagating according to the one-dimensional inviscid Burgers equation is given. The formulation relies on the implicit Earnshaw solution and therefore is only valid prior to shock formation. As explicit examples, the slope density evolution of an initially sinusoidal plane wave, initially Gaussian-distributed planar noise, and an initially triangular wave are presented. The triangular wave is used to examine weak-shock limits without violating the theoretical assumptions. It is also shown that the moments of the slope density function as a function of distance may be written as an expansion in terms of the moments of the source slope density function. From this expansion, approximate expressions are presented for the above cases as well as a specific non-Gaussian noise case intended to mimic features of jet noise. Finally, analytical predictions of the propagation of initially Gaussian-distributed noise are compared favorably with plane-wave tube measurements. © 2016 Acoustical Society of America.

[<http://dx.doi.org/10.1121/1.4941255>]

[PBB]

Pages: 958–967

I. INTRODUCTION

The noise radiated from the complex source represented by high-speed jets has motivated various studies describing its nonlinear propagation. Nonlinearity has been considered in both the geometric near and far fields on jets of different scales. However, the complexities of considering a distributed, stochastic source have prompted study of measures for quantifying nonlinear propagation effects and additional investigations into the theory of nonlinear propagation for arbitrary waveforms. In addition to spectral measures of the effects of nonlinearity (such as frequency-frequency interactions^{1–3} and the quadspectral density of the pressure squared-pressure waveforms^{4–7}), various statistical measures have been proposed, such as the number of zero crossings per unit time,⁸ the average slope at zero crossings,⁹ and the average and wave steepening factors.^{10–12} Other statistical measures are various moments of the amplitude density function or the time-derivative amplitude density function (referred to hereafter as the slope density function) of the waveform of interest. For example, the growth of the skewness of the pressure time derivative waveform, the third standardized central moment of the slope density function, has been shown to be associated with an increase in the pressure waveform shock content.^{13–17} The fourth standardized central moment—the kurtosis—of the waveform derivative has also been calculated in some cases.^{18–20}

While the statistical measures of nonlinearity all depend on the slope density functions of the waveforms of interest, characterizing the density functions themselves has not

received as much attention as the measures of the amplitude density function. Rudenko and Chirkin²¹ and Webster and Blackstock²² showed that the amplitude density function does not vary for plane waves propagating according to the inviscid Burgers equation in the pre-shock region. Additionally, Sakagami *et al.*²³ experimentally found that the density function of initially Gaussian-distributed random noise propagating in a plane-wave tube did not change substantially until after shock formation, and then tended toward a uniform distribution. Those studies that have considered both the slope and amplitude density functions are more recent. McInerny *et al.*²⁴ and Gee *et al.*¹⁹ have shown that the amplitude and slope density functions for jet noise from high-power military aircraft do not follow a Gaussian distribution. Muhlestein and Gee²⁵ experimentally obtained density functions for initially sinusoidal signals and initially Gaussian-distributed noise propagating in a plane-wave tube, and found that the slope density undergoes significant evolution with propagation, while the amplitude density function undergoes minor evolution with propagation. The observed evolution of the slope density function suggests an analytical analysis of the evolution may yield additional insights into the nature of nonlinear noise propagation.

This paper presents an analytical formulation of the evolution of the slope density function (the density function of the first time-derivative of a pressure waveform) for a waveform propagating according to the inviscid Burgers equation and draw some conclusions about the general evolution of moments of the slope density function, in particular, the skewness of the first time derivatives. As examples, the slope density function evolution and a quintic approximation of the evolution of the skewness of the first time derivatives for

^{a)}Electronic mail: mimuhle@gmail.com

initially sinusoidal plane waves and initially Gaussian-distributed noise are derived. Because the present derivation does not assume any particular initial distribution, it provides an analytical comparison for any one-dimensional experimental analysis. This is demonstrated by considering the case of simulated jet noise. Additionally, information about slope densities in the weak shock region is obtained without violating the tenets of the theoretical development by considering the case of an initially triangular waveform as it evolves to a sawtooth. Finally, a comparison of the slope density function for initially Gaussian noise propagated in a plane-wave tube is compared with analytical expressions to validate the analytical derivation.

II. EVOLUTION OF THE SLOPE DENSITY FUNCTION

A. Physical interpretation of the slope density function

We define the slope density function as the probability density function of the first derivative of a time waveform. Any process that affects the shape of a waveform will therefore also affect the slope density of the waveform. For example, thermoviscous attenuation of propagating broadband noise attenuates the higher frequencies more than the lower frequencies, effectively smoothing out the time waveform, decreasing the probability of large-magnitude slopes. Quadratic nonlinearity in propagation, on the other hand, tends to increase positive slopes and decrease negative slopes, which causes the slope density function to distort asymmetrically. Additionally, smaller percentages of the waveforms will be associated with the positive slopes while greater percentages of the waveforms will be associated with the negative slopes. Thus, quadratic nonlinearity causes the positive slope densities to become smaller and farther from zero, while the negative slope densities to become larger and closer to zero.

An example of the effect of quadratic nonlinearity on a waveform, its time derivative, and its density functions is shown in Fig. 1. The pressure waveform of an initially sinusoidal plane wave, its time derivative, its amplitude density function, and its slope density function are shown for $\sigma = 0$ and $\sigma = 0.5$, where σ is the distance relative to the shock formation distance. At $\sigma = 0$, half of the pressure waveform (top left) is positively sloped and half is negatively sloped. Notice that the density of the initially sinusoidal pressure waveform (top right) does not change with propagation. As proven by Rudenko and Chirkin²¹ and Webster and Blackstock,²² the amplitude density function remains undisturbed by propagation in the pre-shock region. This insensitivity of the amplitude density to quadratic nonlinearity relative to the slope density is why the statistics of the pressure waveform do not inform concerning nonlinearity in propagation, and why attention is instead given to the statistics of the time derivative of the pressure waveform.

As the initially sinusoidal waveform distorts, the pressure derivative waveform (Fig. 1, bottom left) becomes more “peaked,” as the positive derivatives become larger and have a shorter duration, while the negative derivatives approach zero and have a larger duration. By $\sigma = 0.5$, for instance,

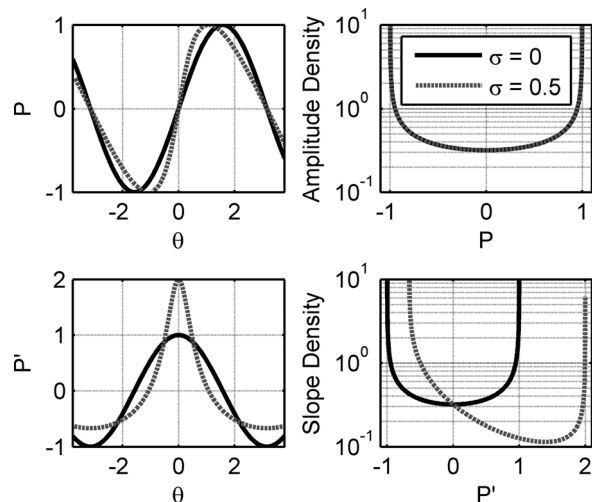


FIG. 1. Time waveform of the normalized pressure P (upper left), derivative of time waveform of the normalized pressure P' (lower left), amplitude density function (upper right), and slope density function (lower right) of an initially sinusoidal plane wave propagating according to the inviscid Burgers equation are plotted as a function of the normalized time θ at the source ($\sigma = 0$) and at half the shock formation distance ($\sigma = 0.5$).

only 34% of the pressure waveform has a positive slope and 66% has a negative slope, and the maximum slope is $P' = 2$ while the minimum slope is $P' = -2/3$. This difference in duration and peak magnitude is exhibited in the slope density (bottom right) as asymmetry about zero. The positive slope densities are much lower than the negative slope densities, but the positive slope densities also extend to much higher magnitudes than the negative slope densities.

B. Derivation of the slope density function evolution

As discussed and shown in the sinusoidal example, the amplitude density function remains constant in the pre-shock region, while the slope density function evolves. In this section, the evolution of the slope density function for progressive plane waves due to quadratic nonlinearity is derived using the (implicit) Earnshaw solution to the inviscid Burgers equation.²⁶ The Earnshaw solution may be written as

$$p = p_s(\phi),$$

$$\phi = \tau + \frac{\beta}{\rho_0 c_0^3} p_s(\phi) x, \quad (1)$$

where p is the acoustic pressure, $p_s(t)$ is the pressure function at the source, ϕ is the Earnshaw phase variable, τ is the retarded time, x is the distance from the source, c_0 is the small-signal sound speed, β is the coefficient of nonlinearity, and ρ_0 is the ambient density.²⁶ Equation (1) is valid while the waveform remains continuous, i.e., until the first shock forms. The shock formation distance, \bar{x} , is defined as the distance x at which the time of arrival first becomes non-monotonic, which occurs at $\bar{x} = \rho_0 c_0^3 / \beta \max\{p'_s(t)\}$, where the prime denotes differentiation with respect to the argument. If we define $\eta = \beta / \rho_0 c_0^3$, Eq. (1) may be written parametrically as

$$(\tau, p) = (\phi - \eta x p_s(\phi), p_s(\phi)), \quad x \leq \bar{x}, \quad (2)$$

which should be read as (retarded time of arrival, pressure amplitude) for distances less than the shock formation distance.

If we let p_0 and τ_0 be a characteristic amplitude and time scale for the initial waveform, then we may define the dimensionless quantities $\sigma = \eta p_0 x / \tau_0$, $\theta = \phi / \tau_0$, and $P_s = p_s / p_0$. We emphasize that p_0 and τ_0 are only characteristic, and $\sigma = 1$ does not necessarily correspond to shock formation. This choice is made anticipating initially random waveforms, where the shock formation distance is unique for each waveform realization. With the present definitions, the shock formation distance becomes $\bar{\sigma} = \max\{1/P'_s(\theta)\}$. Thus we may write Eq. (2) as

$$(\Theta, P) = (\theta - \sigma P_s(\theta), P_s(\theta)), \quad \sigma \leq \bar{\sigma},$$

where Θ and P are the normalized retarded time of arrival and the normalized pressure amplitude, respectively. A schematic interpretation of this parametric solution is shown in Fig. 2. Now, for a given σ , consider the wave amplitude at θ and $\theta + \Delta\theta$, for $\Delta\theta > 0$. The difference in normalized arrival times is

$$\begin{aligned} \Theta(\theta + \Delta\theta) - \Theta(\theta) &= (\theta + \Delta\theta - \sigma P_s(\theta + \Delta\theta)) - (\theta - \sigma P_s(\theta)) \\ &= \Delta\theta - \sigma(P_s(\theta + \Delta\theta) - P_s(\theta)), \end{aligned}$$

and the difference in the normalized pressure amplitudes is

$$P(\theta + \Delta\theta) - P(\theta) = P_s(\theta + \Delta\theta) - P_s(\theta).$$

If we take the ratio of the pressure and arrival time differences and let $\Delta\theta \rightarrow 0$, we find that

$$(\Theta, P') = \left(\theta - \sigma P_s(\theta), \frac{P'_s(\theta)}{1 - \sigma P'_s(\theta)} \right), \quad \sigma \leq \bar{\sigma}, \quad (3)$$

which should be read as (normalized retarded time of arrival, normalized pressure amplitude slope).

When analyzing Eq. (3), one may notice that a given time interval varies with distance depending on the function. For example, the intervals between times of arrival in Fig. 2 are equal at the source but become irregular after

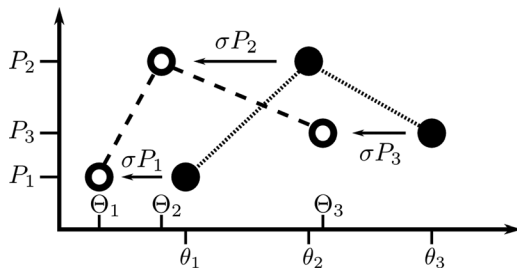


FIG. 2. Schematic explanation of the Earnshaw solution: three points of a pressure waveform P_i with retarded arrival times θ_i at the source and retarded arrival times Θ_i after propagating a distance σ .

propagation. In fact, an infinitesimal normalized time interval may be written

$$d\Theta = d\theta - \sigma P'_s d\theta = d\theta(1 - \sigma P'_s), \quad (4)$$

where the dependence of P'_s on θ has been suppressed. Then, any infinitesimal time interval $d\Theta$ expands or contracts by a factor of $1 - \sigma P'_s$ by the distance σ . Since the slope over the infinitesimal time interval $d\Theta$ may be considered constant at a given location, the probability of measuring the slope P' at a distance σ is the same as the probability of measuring the slope P'_s at the source multiplied by $1 - \sigma P'_s(\theta)$.

Since it is a probability density function, $\rho(P')dP'$ is the fraction of the waveform having a slope between P' and $P' + dP'$. Then, from the arguments made regarding Eq. (3), we may write

$$\rho_\sigma(P')dP' = \rho_0(P'_s)dP'_s(1 - \sigma P'_s). \quad (5)$$

Solving Eq. (3) for P'_s and substituting into Eq. (5), we conclude

$$\rho_\sigma(P')dP' = \rho_0 \left(\frac{P'}{1 + \sigma P'} \right) \frac{dP'}{(1 + \sigma P')^3}, \quad (6)$$

which indicates the slope density may be written as

$$\rho_\sigma(P') = \rho_0 \left(\frac{P'}{1 + \sigma P'} \right) \frac{1}{(1 + \sigma P')^3}. \quad (7)$$

Because this derivation is based on the Earnshaw solution without reference to any form of shock theory, the results are invalid once a slope has become infinite. If the maximum possible slope in a source waveform is $P'_{s,\max} < \infty$, then we find the slope density in Eq. (7) is valid for $\sigma < 1/P'_{s,\max}$, and the domain of $\rho_\sigma(P')$ can be written as $(-1/\sigma, P'_{s,\max}/[1 - \sigma P'_{s,\max}])$. There is a subtlety in this restriction that becomes important when considering Gaussian-distributed noise. Since a Gaussian distribution never goes exactly to zero, there is no finite slope that may be considered the “maximum possible slope,” and the shock formation distance goes to zero. Therefore, when considering an idealized truly Gaussian distributed waveform, any results obtained for $\sigma > 0$ must be only approximate, as some percentage of the waveform has already been affected by shocks. In practice, however, this is not a problem because any finite-sampled, bandlimited source waveform cannot be truly Gaussian distributed and will have a finite maximum slope and a non-zero shock formation distance. Thus, for small σ the approximation is very good, though what “small” means depends on the waveform.

Notice that Eq. (7) depends only on the source slope density and the dimensionless distance, σ . This means the slope density and its various moments are independent of frequency content. Therefore, the evolution of sine waves with different frequencies or of narrow and broadband noise with the same source slope density can only differ after shocks form.

Because several measures that quantify nonlinearity rely on moments of the slope density, it is useful to examine how

these moments evolve according to the present theory. Since we assume an acoustic process has a zero-mean time derivative, the n th (central) moment²⁷ may be written as

$$\begin{aligned}\mu_\sigma^{(n)} &= \int_a^b (P')^n \rho_\sigma(P') dP' \\ &= \int_{-\infty}^{P'_{s,\max}} \rho_0(P'_s) \frac{(P'_s)^n dP'_s}{(1 - \sigma P'_s)^{n-1}},\end{aligned}\quad (8)$$

where $a = -1/\sigma$ and $b = P'_{s,\max}/(1 - \sigma P'_{s,\max})$. The change of the integrand comes from Eq. (6) and the change of limits comes from moving from integrating over P' to P'_s [see Eq. (3)]. If the slope density function is properly normalized, we should find $\mu_\sigma^{(0)} = 1$. To check this, we may write

$$\mu_\sigma^{(0)} = \int_{-\infty}^{P'_{s,\max}} [\rho_0(P'_s) - \sigma P'_s \rho_0(P'_s)] dP'_s = \mu_0^{(0)} - \sigma \mu_0^{(1)}.\quad (9)$$

Since $\mu_0^{(0)} = 1$ by definition, the slope density function is properly normalized if the average slope is zero, which is the case for acoustic signals.

The last integral in Eq. (8) is similar to the definition of the n th central moment of the initial distribution except for the denominator. For small σ (such that $|\sigma P'_s| < 1$ for the entire interval), we may expand the denominator as a power series in $\sigma P'_s$, which becomes a series of moments of the source slope density

$$\mu_\sigma^{(n)} = \sum_{k=0}^{\infty} \frac{(n-2+k)!}{(n-2)!k!} \mu_0^{(n+k)} \sigma^k.\quad (10)$$

As mentioned in Sec. I, the skewness of the time-derivative of a waveform, or derivative skewness, has been used in nonlinear noise analysis. From Eq. (10), we may estimate the derivative skewness of a propagating wave very close to the source ($\sigma \ll 1$) to be

$$\begin{aligned}\text{Sk}(P') &= \frac{\mu_0^{(3)}}{(\mu_0^{(2)})^{3/2}} + \frac{4\mu_0^{(2)}\mu_0^{(4)} - 3(\mu_0^{(3)})^2}{2(\mu_0^{(2)})^{5/2}} \sigma \\ &+ \frac{15(\mu_0^{(3)})^3 - 36\mu_0^{(2)}\mu_0^{(3)}\mu_0^{(4)} + 24(\mu_0^{(2)})^2\mu_0^{(5)}}{8(\mu_0^{(2)})^{7/2}} \sigma^2 \\ &+ O(\sigma^3).\end{aligned}\quad (11)$$

The first term in Eq. (11) is just the derivative skewness of the initial distribution. The linear term depends only on the second, third, and fourth source moments, and the quadratic term depends only on the second through fifth moments. Notice that each term in the constant and the quadratic coefficients includes a source moment with an odd number. This is general for all coefficients of even powers of σ . Thus, in the special case of an initially symmetric slope density (e.g., Gaussian and sinusoidal distributions), the coefficients of all even powers of σ are zero, and we may simplify the expression of the derivative skewness to

$$\begin{aligned}\text{Sk}(P') &= \frac{2\mu_0^{(4)}}{(\mu_0^{(2)})^{3/2}} \sigma + \frac{4\mu_0^{(2)}\mu_0^{(6)} - 3(\mu_0^{(4)})^2}{(\mu_0^{(2)})^{5/2}} \sigma^3 \\ &+ \frac{15(\mu_0^{(4)})^3 - 36\mu_0^{(2)}\mu_0^{(4)}\mu_0^{(6)} + 24(\mu_0^{(2)})^2\mu_0^{(8)}}{4(\mu_0^{(2)})^{7/2}} \sigma^5 \\ &+ O(\sigma^7).\end{aligned}\quad (12)$$

Because the Burgers equation for cylindrical and spherical outward-progressive waves may also be reduced to the planar equation through a change in variables, the same methodology can be used to produce slope density functions and moment expansions for these other one-dimensional systems. For example, the slope density function for a spherically propagating wave is

$$\rho_{\sigma_s}(P') = \rho_0 \left(\frac{P'}{e^{-\sigma_s/\eta_s} + \sigma_s P'} \right) \frac{1}{(1 + \sigma_s P' e^{\sigma_s/\eta_s})^3},\quad (13)$$

where $\rho_0(P')$ is the slope density function at a reference radius r_0 , $\sigma_s = \eta_s \ln(r/r_0)$ is a non-dimensional distance, $\eta_s = \eta p_0 r_0 / \tau_0$, r is the radius, and p_0 and τ_0 are now the characteristic amplitude and time scale of the waveform at the reference radius. Similarly, the moments as functions at a radius of r may be written in the form of a power series as

$$\mu_{\sigma_s}^{(n)} = e^{-n\sigma_s/\eta_s} \sum_{k=0}^{\infty} \frac{(n-2+k)!}{(n-2)!k!} \mu_{r_0}^{(n+k)} \sigma_s^k.\quad (14)$$

Equation (14) is the same as Eq. (10) except that it is multiplied by an exponential term. Since the derivative skewness is $\mu_{\sigma_s}^{(3)}/(\mu_{\sigma_s}^{(2)})^{3/2}$, the exponential factors cancel, and Eqs. (11) and (12) may be used if $\mu_0^{(n)}$ and σ are replaced by $\mu_{r_0}^{(n)}$ and σ_s , respectively.

III. EXAMPLES OF SLOPE DENSITY

A. Initial sinusoid

An important benchmark case in nonlinear acoustics is the propagation of an initially sinusoidal signal. Exact solutions for the evolution of the waveform for all $\sigma > 0$ are given by the Fubini solution and the Blackstock bridging function.²⁸ In addition, exact values of the derivative skewness¹⁷ and average or wave steepening factor,¹⁰ which are associated with the moments of the slope density, exist for all $\sigma > 0$. However, the slope density of the initially sinusoidal signal itself has not yet been explicitly considered. Therefore, we present an analysis here.

Consider a sinusoidal source condition with angular frequency, ω , and amplitude, p_0 . With these conditions, we choose p_0 for our characteristic amplitude and $1/\omega$ as the characteristic time scale, such that $\bar{\sigma} = 1$.²⁶ Then, since the derivative of a sinusoid is also a sinusoid, the slope density of the waveform at the source $\rho_{0,\text{sine}}(P')$ may be written²⁷

$$\rho_{0,\text{ sine}}(P'_s) = \begin{cases} [\pi\sqrt{1-P_s'^2}]^{-1}, & -1 < P'_s < 1, \\ 0, & \text{otherwise.} \end{cases} \quad (15)$$

Therefore, the slope density at σ is

$$\rho_{\sigma,\text{ sine}}(P') = \rho_{0,\text{ sine}}\left(\frac{P'}{1+\sigma P'}\right) \frac{1}{(1+\sigma P')^3} = \begin{cases} \left[(1+\sigma P')^2 \sqrt{(1+\sigma P')^2 - P'^2} \right]^{-1}, & -\frac{1}{1+\sigma} < P' < \frac{1}{1-\sigma}, \\ 0, & \text{otherwise.} \end{cases} \quad (16)$$

The slope density at several values of σ are shown in Fig. 3, which expands the slope density function shown in Fig. 1. For all $\sigma < 1$ the distribution consists of two peaks that rise rapidly to infinity, relatively low values between the peaks, and is exactly zero beyond the peaks. The slope at which the negative peak occurs approaches zero and the slope at which the positive peak occurs moves farther from zero as σ increases. At $\sigma = 1$ the positive peak has moved all the way to $P' \rightarrow \infty$, which indicates the generation of a shock. Notice the slopes between the two peaks tend to decrease in probability with increasing slope amplitude, indicative of the lower percentage of the waveform with positive slopes.

The even moments of the source slope density (the odd moments are all zero) may be written as

$$\mu_0^{(n)} = \frac{2\Gamma((n+1)/2)}{n\Gamma(n/2)} = \frac{2(n-1)!!}{2^{n/2}(n/2)!n}. \quad (17)$$

Then, using Eq. (12) for $\sigma \ll 1$ we may approximate the derivative skewness as

$$\text{Sk}(P') = \frac{3\sigma}{\sqrt{2}} + \frac{13\sigma^3}{32\sqrt{2}} + \frac{165\sigma^5}{128\sqrt{2}} + O(\sigma^7). \quad (18)$$

This matches to fifth-order an expansion of the exact form of the derivative skewness found by Muhlestein.¹⁷ A plot of the

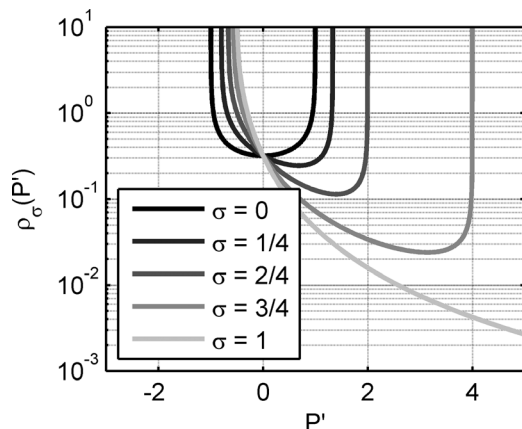


FIG. 3. Probability density function of the normalized time-derivative amplitudes of an initially sinusoidal signal at various values of the normalized distance σ .

exact derivative skewness as a function of σ is plotted in Fig. 4 with the linear, cubic, and quintic order approximations as given in Eq. (18). As seen in Fig. 4, all three of the approximations diverge rather quickly as $\sigma \rightarrow 1$. In fact, the linear, cubic, and quintic approximations have less than a 10% error relative to the exact solution only up to $\sigma = 0.42, 0.47,$ and $0.52,$ respectively.

B. Gaussian noise

The second example of slope density evolution is that of Gaussian-distributed noise. To describe the slope-density evolution of Gaussian noise analytically, it is convenient to define the standard deviation of the source slope density, $\sqrt{\mu_0^{(2)}}$, as the characteristic slope density s_0 , the characteristic pressure amplitude as p_0 . These definitions require the characteristic time scale to be $\tau_0 = p_0/s$, which in turn means $\sigma = \eta s x$. The Gaussian noise slope density function may then be written as

$$\rho_{0,\text{ Gauss}}(P'_s) = \frac{e^{-(P'_s)^2/2}}{\sqrt{2\pi}}. \quad (19)$$

As discussed in Sec. II B, the initial Gaussian slope density in Eq. (19) is nonzero for every finite slope value at the source, we find shock content to exist in the noise for all

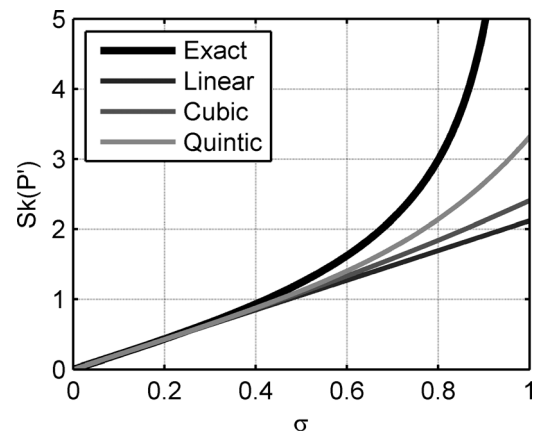


FIG. 4. Exact skewness of first time derivative of an initially sinusoidal signal. The linear, cubic, and quintic approximations of the analytical expression are shown for comparison. The shock formation distance is $\sigma = 1$.

$\sigma > 0$; in other words, $\bar{\sigma} = 0$. However, in practice finite waveforms cannot have truly Gaussian distributed slopes, and shocks are not likely to appear in the source waveform, and a nonzero value of $\bar{\sigma}$ may be found. In this case, the initial Gaussian distribution is already an approximation, though it may be a very good one. As an example, if a pressure derivative waveform follows a Gaussian distribution out to four standard deviations and then abruptly goes to zero, the shock formation distance would be $\bar{\sigma} = 0.25$, and the correction to the initial slope distribution would be $O(1 - \text{erf}[4/\sqrt{2}]) \approx O(6 \times 10^{-5})$.

The slope density for initially Gaussian noise at a distance σ is approximately

$$\rho_{\sigma, \text{Gauss}}(P') \approx \exp\left[-\frac{1}{2}\left(\frac{P'}{1 + \sigma P'}\right)^2\right] \frac{H(P' + \sigma^{-1})}{\sqrt{2\pi}(1 + \sigma P')^3}, \quad (20)$$

where $H(x)$ is the Heaviside function. The slope density is plotted for several values of σ in Fig. 5. The even moments of the source distribution (the odd moments are all zero) may be written as

$$\mu_0^{(n)} = (n - 1)!! \quad (21)$$

Then, using Eq. (12) for $\sigma \ll 1$ we may write the derivative skewness as

$$\text{Sk}(P') = 6\sigma + 33\sigma^3 + \frac{2115}{4}\sigma^5 + O(\sigma^7). \quad (22)$$

In order to understand the accuracy of this estimate, the derivative skewness of a numerically-propagated initially Gaussian-distributed (finite time and bandlimited) noise waveform is compared with the analytical formulation in Fig. 6. The characteristic amplitude of the numerical waveform is set to be $p_0 = 10$ Pa and the characteristic slope amplitude is $s_0 = 183$ kPa/s, leading to a characteristic time scale of $\tau = 54.5 \mu\text{s}$. The source passband is chosen to be 500–2000 Hz, rolling off according to a fourth-order Butterworth filter. For this particular waveform realization,

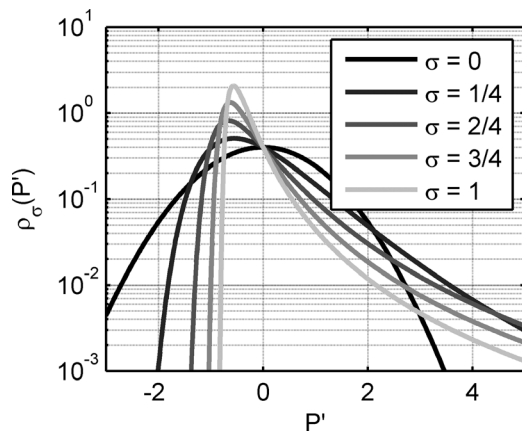


FIG. 5. Probability density function of the normalized time-derivative amplitudes of initially Gaussian noise at various values of the normalized distance σ . As discussed, $\sigma = 1$ does not correspond to shock formation.

the shock formation distance, or the distance at which the first discontinuity forms in a given noise waveform, is approximately $\sigma = 0.21$. The sampling rate, chosen to match the experimental setup described in Sec. IV, was $4.9 \mu\text{s}/\text{sample}$ (204 800 Hz) and 2^{18} samples were used. The waveform was propagated using a mixed time-frequency domain code developed by Gee *et al.*⁶ Linear, cubic, and quintic polynomial truncations of the analytical formulation [see Eq. (22)] are shown for comparison. Qualitatively, the linear polynomial predicts the derivative skewness of our particular noise waveform well (relative error $< 10\%$) out to $\sigma \approx 0.05$, the cubic polynomial predicts well out to $\sigma \approx 0.07$, and the quintic polynomial predicts well out to $\sigma \approx 0.08$.

A brief note on the sampling rate and its effect on the derivative skewness is in order. Once a shock has formed in a waveform, regardless of where or how many are present, $\text{Sk}(P')$ of a continuously sampled waveform goes to infinity. However, with a finite sampling rate, a single shock in the waveform will not have nearly as dramatic effect on $\text{Sk}(P')$. For this case, the ratio of the sampling rate to the peak relevant frequency for the numerical data in Fig. 6 is about 100, which was shown by Gee *et al.*,²⁹ to yield reasonable predictions for an initially sinusoidal waveform up to $\text{Sk}(P') \approx 5$, after which point the predicted derivative skewness approaches a constant and underestimates the true derivative skewness. Thus, the derivative skewness of the waveform in the neighborhood of the shock is “saturated” due to finite sampling rates, and the predicted derivative skewness of the entire waveform does not become infinite at the shock formation distance $\sigma = 0.21$. On the other hand, the vast majority of the positive slopes in the waveform have not yet formed shock waves, and so the derivative skewness overall continues to increase. Therefore, for finite sampling rates $\text{Sk}(P')$ may be best described as a characteristic value rather than an exact value.

C. Non-Gaussian noise

The initial sinusoidal signal and initial Gaussian-distributed noise are examples of symmetric initial slope densities, but not all sources of high-amplitude sound are symmetric. An

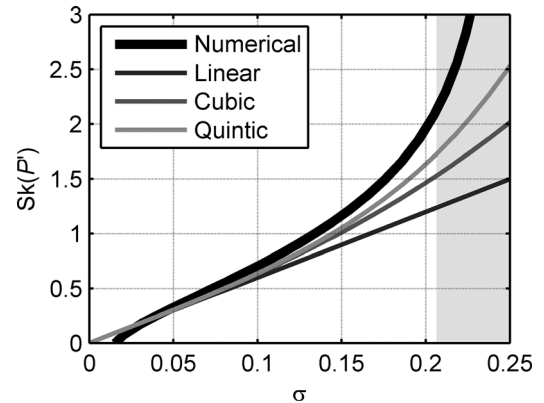


FIG. 6. Skewness of first time derivative of Gaussian-distributed noise numerically propagated according to the Earnshaw solution. The linear, cubic, and quintic approximations of the analytical expression are shown for comparison. The gray backgrounds denote distances after shock formation.

important example is supersonic jets, such as those associated with rockets and military aircraft; near-field measurements reveal a positively skewed slope density.^{18,19} Using just the published values of the derivative skewness and derivative kurtosis at an initial measurement distance allows us to make some comments about the evolution of the derivative skewness for this non-Gaussian noise example.

The derivative skewness of an arbitrary initial waveform is given in Eq. (11) in terms of the initial central moments. We may in turn write Eq. (11) in terms of the standardized moments as

$$\text{Sk}(P') = \text{Sk}(P'_s) + \left[2\text{Kt}(P'_s) - \frac{3}{2}\text{Sk}(P'_s) \right] s_0 \sigma + O((s_0 \sigma)^2),$$

where $\text{Kt}(P'_s)$ is the derivative kurtosis at the source and s_0 is the source slope standard deviation. If we again choose s_0 to be the characteristic slope amplitude and τ_0 to be the characteristic time scale, we may then write

$$\text{Sk}(P') = \text{Sk}(P'_s) + \left[2\text{Kt}(P'_s) - \frac{3}{2}\text{Sk}(P'_s) \right] \sigma + O(\sigma^3). \quad (23)$$

Scale-model measurements suggest the derivative skewness and kurtosis are about 1 and 4 for jet noise near the shear layer,^{20,30} as compared to 0 and 3 for Gaussian-distributed noise. If we approximate only to linear order, Eq. (23) suggests the derivative skewness may be written as

$$\text{Sk}(P') = 1 + 6.5\sigma + O(\sigma^2). \quad (24)$$

In addition to starting higher than initially Gaussian noise, we see the derivative skewness of jet noise grows more rapidly near the source as well. While further knowledge of the initial slope density is required to extend the analysis to higher than linear orders of σ , this analysis suggests jet noise may steepen more quickly than initially Gaussian noise.

D. Triangle and sawtooth waves

As discussed above, the description of the slope density evolution presented in Sec. II B cannot account for the propagation of shock waves. However, far after the shock formation distance weak shock theory predicts an initially sinusoidal signal will approach a sawtooth waveform²⁶ and initially Gaussian noise will approach a similar state, consisting of perfect shocks connected by straight waveform segments with a uniform slope.^{9,31,32} We may obtain some insight into the nature of the slope density function in this limit by considering the propagation of an initially triangular function to shock formation, where the continuous waveform immediately becomes a sawtooth (see Fig. 7).

The slope density of the initial triangle wave may be written as

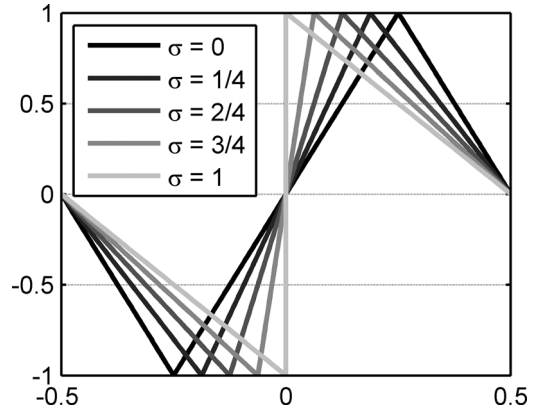


FIG. 7. Pressure waveform of an initially triangular waveform at various distances from the source $\sigma=0$ to the shock formation distance $\sigma=1$.

$$\rho_{0,\Delta}(P'_s) = \frac{\delta(P'_s + 1) + \delta(P'_s - 1)}{2}, \quad (25)$$

where $\delta(P')$ is the Dirac δ -function and the characteristic slope is the amplitude of the triangle wave divided by a quarter of a period. Then, the slope density at farther distances is written as

$$\rho_{\sigma,\Delta}(P') = \frac{1}{2(1 + \sigma P')^3} \left[\delta\left(\frac{P'}{1 + \sigma P'} + 1\right) + \delta\left(\frac{P'}{1 + \sigma P'} - 1\right) \right]. \quad (26)$$

Therefore $\bar{\sigma} = 1$. The argument of the δ -functions are equal to zero at $P' = -1/(1 + \sigma)$ or at $P' = 1/(1 - \sigma)$. Thus, from the identity

$$\delta(g(x)) = \sum_i \frac{\delta(x - x_i)}{|g'(x_i)|}, \quad (27)$$

where x_i is the i th zero crossing of $g(x)$, we may write

$$\rho_{\sigma,\Delta}(P') = \frac{1 + \sigma}{2} \delta\left(P' + \frac{1}{1 + \sigma}\right) + \frac{1 - \sigma}{2} \delta\left(P' - \frac{1}{1 - \sigma}\right). \quad (28)$$

Thus, in the limit that $\sigma \rightarrow 1$ and the triangle wave becomes a sawtooth, we find that there is a δ -function at $P' = -1/2$ with amplitude 1, and a δ -function at positive infinity ($P' = \lim_{\sigma \rightarrow 1} (1 - \sigma)^{-1}$) with amplitude zero. Since the slope density function of an initially triangular wave is written in terms of Dirac δ -functions, we may also calculate the derivative skewness exactly

$$\text{Sk}(P') = \frac{2\sigma}{\sqrt{1 - \sigma^2}}. \quad (29)$$

As mentioned above, the primary motivation for studying the initially triangular wave is to compare with the weak-shock propagation regime of other initial waveforms. For an initially sinusoidal plane wave, the connection may

be made explicitly. Initially sinusoidal plane waves propagating without linear losses approach the sawtooth wave of the form²⁶

$$P = \frac{\pi - \theta}{1 + \sigma} \quad 0 < \theta < 2\pi, \quad (30)$$

where the normalization amplitude and time scale are p_0 and ω^{-1} , respectively. This means that the slope density in the weak-shock propagation regime is

$$\rho_{\text{saw},\sigma}(P') = \delta\left(P' + \frac{1}{1 + \sigma}\right) + \frac{1}{2} \lim_{\sigma \rightarrow 1} (1 - \sigma) \delta\left(P' - (1 - \sigma)^{-1}\right). \quad (31)$$

Thus, in the limit that the distance from the source is much farther than a shock formation distance, the slope density of the initial sinusoidal signal may be considered to have two “peaks,” one at $-1/(1 + \sigma)$ with probability of 1 and one at infinity with 0 probability. Intuitively, this is expected, since the slope density of a sine wave has two peaks, and as it propagates the negative peak moves closer to zero and the positive peak moves toward infinity. The analysis of the initial triangular wave simply implies that this general shape continues for the entire propagation.

Less intuitively, the slope density of initially Gaussian-distributed noise will also approach the slope density of an initially triangular wave at shock formation. While the initial slope density has only a single peak, after a long distance of propagation, all of the positive slopes will be infinitely thin and sharp and all of the negative slopes will take the same value, similar to a sawtooth wave.^{9,31,32} On the other hand, even though the initially Gaussian-distributed noise will approach the same slope density as the initially sinusoidal signal, the evolution of these two initial cases toward the ultimate limit are very different. Using the present analysis, however, we cannot comment on the differences between the two cases.

IV. EXPERIMENTAL VERIFICATION

In order to analyze the validity of the analytical method derived in Sec. II B, we may compare the predicted slope densities with the measured slope densities from a plane-wave tube experiment. The experimental setup is fully described in Muhlestein *et al.*¹⁰ The tube consisted of several 3.05 m (10 ft) segments of PVC pipe connected end to end with PVC couplers. The inner diameter of the tube was 5.08 cm (2 in). The tube was driven at one end by a BMS (Hanover, Germany) 4590 coaxial compression driver and was terminated anechoically with about a meter long piece of fiber-glass insulation at the other end. Microphone holes were drilled in the tube 0.4, 2.6, and 5.6 m from the driver. The holes were designed such that the diaphragms of the microphones were flush with the inner tube wall and were fit snugly. The microphones were 3.18 mm (1/8 in) 40DD G.R.A.S. (Holte, Denmark) pressure microphones without grid caps. Measurements were taken at 204 800 Hz for 5 s. The input waveform was an initially Gaussian-distributed signal (0.7–2.4 kHz, based on 3 dB-down points) with an

amplitude standard deviation of 620 Pa and a slope standard deviation of 5.9 MPa/s at the first microphone. Thus, using the definition of σ in Sec. III B, we may write the shock formation distance as about $\bar{\sigma} = 0.15$, and the normalized distance is given by $\sigma = (0.17 \text{ m}^{-1})x$.

Portions of the measured waveforms are shown in Fig. 8. General waveform steepening is evident by $\sigma = 0.43$ and several shocks are apparent by $\sigma = 0.96$. Since $\bar{\sigma} = 0.15$, at least one shock would exist somewhere in the waveform by $\sigma = 0.43$ (the second measurement location) if the propagation were lossless. Since the analytical predictions are restricted to the pre-shock propagation regime, we do not expect the data from the $\sigma = 0.96$ microphone to agree with predictions.

The slope densities estimated from the measured waveforms are plotted in Fig. 9. The time derivatives of the waveforms were estimated using a forward-difference scheme, and the slope densities were estimated using the “hist” MATLAB[®] function and normalizing. The analytical prediction of the slope densities from Eq. (20) are plotted as well for comparison.

The measured densities shown in Fig. 9 follow the general trend predicted by the analytical solution. In particular, the measured slope densities and the predicted slope densities at $\sigma = 0.06$ and 0.43 have very similar shapes—they both peak in the negative slopes and fall off quickly for large magnitude negative slopes and fall off more slowly for large magnitude positive slopes. While the measured slope density and the analytical prediction differ somewhat in details (for instance, the predicted peak at $\sigma = 0.43$ is at $P' = -0.4$, while the measured peak is at $P' = -0.7$, and the large magnitude probability fall-offs are slightly different), the overall agreement at $\sigma = 0.06$ and 0.43 is quite good. At $\sigma = 0.96$, however, the predicted and measured shapes are quite different. The most likely reason is the presence of “ringing” in the measured data (similar ringing was seen by Pestorius and Blackstock³³ and Falco *et al.*⁵ in their measurements). As a verification of this hypothesis, the waveform measured at

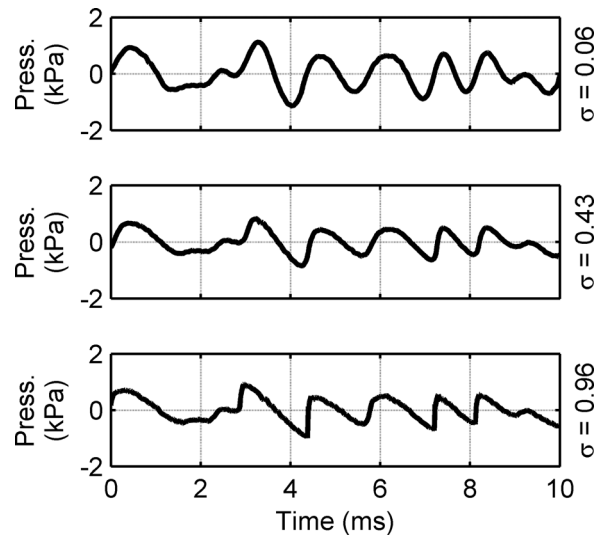


FIG. 8. Broadband (0.7–2.3 kHz) noise waveforms measured 0.4, 2.6, and 5.6 m ($\sigma = 0.06, 0.43, 0.96$) from the source in a plane-wave tube.

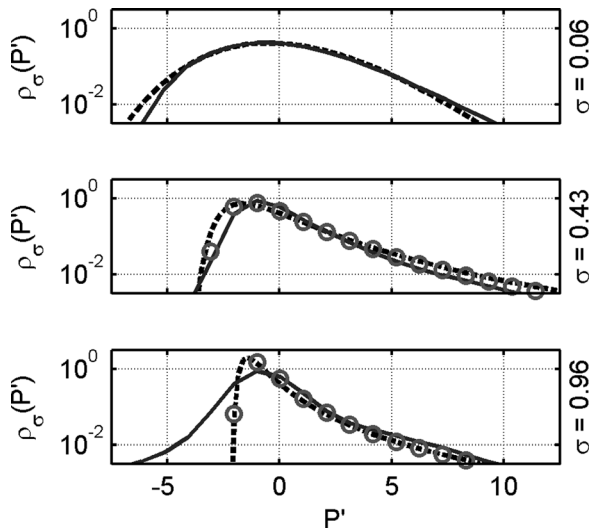


FIG. 9. Slope density functions estimated from the time waveforms shown in Fig. 8 (solid gray lines). The analytical slope density predictions from Eq. (20) (dashed black lines) are plotted for comparison. The open circles are the slope density prediction obtained by numerically propagating the waveform measured at $\sigma = 0.06$ to the farther microphone locations.

$\sigma = 0.06$ was numerically propagated to the other two measurement locations. The slope densities of these predicted waveforms are also shown in Fig. 9 as open circles. As can be seen, the agreement between the analytically and numerically predicted slope densities is better, especially at $\sigma = 0.96$. This agreement may be unexpected, since the theoretical prediction does not account for any form of linear absorption or dispersion processes while the numerical prediction (and, obviously, the experimental measurement) does.

V. CONCLUSIONS

The evolution of the probability density function of the time-derivative of a pressure waveform (slope density) propagating according to the inviscid Burgers equation as a function of the distance from the source based on the source slope density has been derived. This formulation may be used to calculate or estimate the evolution of various metrics of the importance of nonlinearity in sound propagation, such as the skewness of the time derivative of the pressure waveform or the average steepening factor, for a broad set of possible source conditions.

As demonstrations of applying the presented analysis, the slope density of initially sinusoidal, Gaussian-distributed, and triangular waveforms have been derived. The analysis of the initially triangular waveform, which evolves to a sawtooth at shock formation, gives an asymptotic limit to the form of the slope density far past shock formation. As an example of an asymmetric initial slope density, jet noise has been briefly discussed, and it was found the skewness of the slope density increases more rapidly for jet noise than for initially Gaussian-distributed noise. Finally, the analytical predictions were compared with experimentally obtained slope densities, and relatively good agreement was found despite the theory not accounting for the effects of absorption or dispersion in a plane-wave tube environment.

ACKNOWLEDGMENTS

The authors would like to acknowledge the anonymous reviewers, whose useful and supportive comments helped this paper become a more lucid and mature document.

- ¹D. F. Pernet and R. C. Payne, "Non-linear propagation of signals in air," *J. Sound Vib.* **17**, 383–396 (1971).
- ²O. V. Rudenko, "Interactions of intense noise waves," *Sov. Phys. Usp.* **29** 413–447 (1986).
- ³G. P. Howell and C. L. Morfey, "Non-linear propagation of broadband noise signals," *J. Sound Vib.* **114**, 189–201 (1987).
- ⁴L. E. Falco, K. L. Gee, A. A. Atchley, and V. W. Sparrow, "Investigation of a single-point nonlinearity indicator in one-dimensional propagation," Forum Acusticum, Budapest (2005), paper 703, pp. 1385–1389.
- ⁵L. E. Falco, A. A. Atchley, and K. L. Gee, "Investigation of a single-point nonlinearity indicator in the propagation of high-amplitude noise," AIAA Paper 2006-2529 (2006).
- ⁶K. L. Gee, T. B. Gabrielson, A. A. Atchley, and V. W. Sparrow, "Preliminary analysis of nonlinearity in military jet aircraft noise propagation," *AIAA J.* **43**, 1398–1401 (2005).
- ⁷B. O. Reichman, K. L. Gee, T. B. Neilsen, J. J. Thaden, and M. M. James, "Comparison of nonlinear, geometric, and absorptive effects in high-amplitude jet noise propagation," *J. Acoust. Soc. Am.* **136**, 2102 (2014).
- ⁸W. J. Baars, C. E. Tinney, and M. S. Wochner, "Nonlinear noise propagation from a fully expanded Mach 3 jet," AIAA Paper 2012-1177 (2012).
- ⁹Y. Watanabe and Y. Urabe, "Changes of zero-crossing slopes of a finite-amplitude noise propagating in a tube," in *Proceedings of 1st Symposium on Ultrasonic Electronics*, Vol. 20 (1980), Supplement 20-3, pp. 35–39.
- ¹⁰M. B. Muhlestein, K. L. Gee, T. B. Neilsen, and D. C. Thomas, "Evolution of the average steepening factor for nonlinearly propagating waves," *J. Acoust. Soc. Am.* **137**, 640–650 (2015).
- ¹¹J. Gallagher, "The effect of non-linear propagation in jet noise," *20th Aerospace Sciences Meeting and Exhibit*, Orlando, FL, AIAA Paper 82-0416 (1982).
- ¹²W. J. Baars and C. E. Tinney, "Shock structures in the acoustic field of a Mach 3 jet with crackle," *J. Sound Vib.* **333**, 2539–2553 (2014).
- ¹³S. A. McNerny and S. M. Ölçmen, "High-intensity rocket noise: Nonlinear propagation, atmospheric absorption, and characterization," *J. Acoust. Soc. Am.* **117**, 578–591 (2005).
- ¹⁴M. R. Shepherd, K. L. Gee, and A. D. Hanford, "Evolution of statistical properties for a nonlinearly propagating sinusoid," *J. Acoust. Soc. Am.* **130**, EL8–EL13 (2011).
- ¹⁵K. L. Gee, T. B. Neilsen, J. M. Downing, M. M. James, and S. A. McNerny, "Characterizing nonlinearity in military jet aircraft flyover data," *Proc. Mtgs. Acoust.* **12**, 040008 (2013).
- ¹⁶K. L. Gee, T. B. Neilsen, J. M. Downing, M. M. James, R. L. McKinley, R. C. McKinley, and A. T. Wall, "Near-field shock formation in noise propagation from a high-power jet aircraft," *J. Acoust. Soc. Am.* **133**, EL88–EL93 (2013).
- ¹⁷M. B. Muhlestein, *Analyses of Nonlinearity Measures in High-Amplitude Sound Propagation*, Master's thesis, Brigham Young University (2013).
- ¹⁸S. A. McNerny, "Launch vehicle acoustics Part 2: Statistics of the time domain data," *J. Aircraft* **33**, 518–523 (1996).
- ¹⁹K. L. Gee, V. W. Sparrow, A. A. Atchley, and T. Gabrielson, "On the perception of crackle in high-amplitude jet noise," *AIAA J.* **45**, 593–598 (2007).
- ²⁰P. Mora, N. Heeb, J. Kastner, E. J. Gutmark, and K. Kailasanath, "Impact of heat on the pressure skewness and kurtosis in supersonic jets," *AIAA J.* **52**, 777–787 (2014).
- ²¹O. Rudenko and A. Chirkin, "Statistics of discontinuous noise waves in nonlinear media," *Akad. Nauk SSSR Dokl.* **225**, 520–523 (1975).
- ²²D. W. Webster and D. T. Blackstock, "Amplitude density of a finite amplitude wave," *J. Acoust. Soc. Am.* **65**, 1053–1054 (1979).
- ²³K. Sakagami, S. Aoki, I. M. Chou, T. Kamakura, and K. Ikegaya, "Statistical characteristics of finite amplitude acoustic noise propagating in a tube," *J. Acoust. Soc. Jpn. (E)* **3**, 43–45 (1982).
- ²⁴S. A. McNerny, K. L. Gee, M. Downing, and M. M. James, "Acoustical nonlinearities in aircraft flyover data," AIAA Paper 2007-3654 (2007).

- ²⁵M. Muhlestein and K. Gee, "Experimental investigation of a characteristic shock formation distance in finite-amplitude noise propagation," *Proc. Mtgs. Acoust.* **12**, 045002 (2011).
- ²⁶D. T. Blackstock, M. F. Hamilton, and A. D. Pierce, "Progressive waves in lossless and lossy fluids," in *Nonlinear Acoustics* (Acoustical Society of America, New York, 1998) Chap. 4, pp. 65–150.
- ²⁷J. S. Bendat and A. G. Piersol, in *Random Data*, 4th ed. (John Wiley & Sons, Inc., New York, 2010), Chap. 3, pp. 45–78.
- ²⁸D. T. Blackstock, "Connection between the fay and fubini solutions for plane sound waves of finite amplitude," *J. Acoust. Soc. Am.* **39**, 1019–1026 (1966).
- ²⁹K. L. Gee, T. B. Neilsen, A. T. Wall, J. M. Downing, M. M. James, and R. L. McKinley, "Propagation of crackle-containing noise from military jet aircraft," accepted to *Noise Control Eng. J.* **64**(1), 1–12 (2016).
- ³⁰K. L. Gee, T. B. Neilsen, and A. A. Atchley, "Skewness and shock formation in laboratory scale supersonic jet data," *J. Acoust. Soc. Am.* **133**, EL491–EL497 (2013).
- ³¹F. M. Pestorius, S. W. Williams, and D. T. Blackstock, "Effect of nonlinearity on noise propagation," in *2nd Interagency Symposium on University Research in Transportation Noise*, North Carolina State University, Raleigh, NC (1974), pp. 440–460.
- ³²S. N. Gurbatov and A. I. Saichev, "Degeneracy of one-dimensional acoustic turbulence at large Reynolds numbers," *Sov. Phys. JETP* **53**, 347–354 (1981).
- ³³F. Pestorius and D. Blackstock, "Propagation of finite-amplitude noise," *Proceedings of the Symposium on Finite-amplitude Wave Effects in Fluids*, Copenhagen (1974), pp. 24–29.